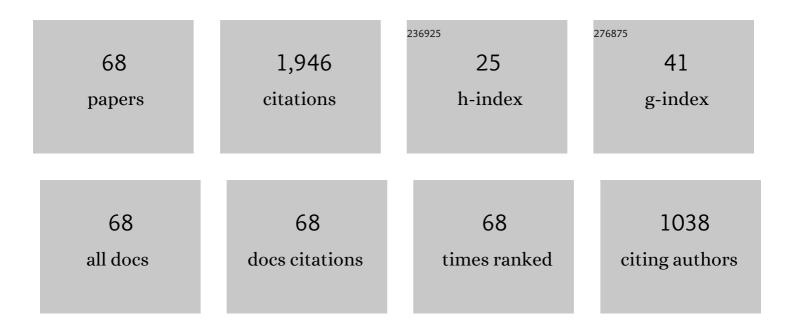
List of Publications by Year in descending order

Source: https://exaly.com/author-pdf/4267749/publications.pdf Version: 2024-02-01



#	Article	IF	CITATIONS
1	Synergistic phosphorized NiFeCo and MXene interaction inspired the formation of high-valence metal sites for efficient oxygen evolution. Journal of Materials Science and Technology, 2022, 106, 90-97.	10.7	35
2	Promoted self-construction of β-NiOOH in amorphous high entropy electrocatalysts for the oxygen evolution reaction. Applied Catalysis B: Environmental, 2022, 301, 120764.	20.2	103
3	Effect of microstructure on temperature dependence of deformation behavior in polycrystalline CoNi-based superalloy. Journal of Materials Science, 2022, 57, 687-699.	3.7	4
4	Analysis of cracks origin behaviors during sulfide stress corrosion (SSC) in HSLA steel at different temperatures by electrochemical noise. Journal of Iron and Steel Research International, 2022, 29, 1836-1845.	2.8	4
5	Metal-organic framework derived dual-metal sites for electroreduction of carbon dioxide to HCOOH. Applied Catalysis B: Environmental, 2022, 311, 121377.	20.2	40
6	Tailoring the tempered microstructure of a novel martensitic heat resistant steel G115 through prior cold deformation and its effect on mechanical properties. Materials Science & Engineering A: Structural Materials: Properties, Microstructure and Processing, 2022, 841, 143015.	5.6	11
7	Enhanced mechanical properties in oxide-dispersion-strengthened alloys achieved via interface segregation of cation dopants. Science China Materials, 2021, 64, 987-998.	6.3	16
8	Nanoscale segregation mechanism of cation dopant at the matrix/oxide interface in oxide dispersion-strengthened alloys. Journal of Materials Science, 2021, 56, 6251-6268.	3.7	2
9	Effects of heat treatment on the microstructure and mechanical properties of Ni3Al-based superalloys: A review. International Journal of Minerals, Metallurgy and Materials, 2021, 28, 553-566.	4.9	19
10	Nano Mo–La–O particles strengthened Mo alloys fabricated via freeze-drying technology and low temperature sintering. Materials Science & Engineering A: Structural Materials: Properties, Microstructure and Processing, 2021, 818, 141448.	5.6	12
11	Self-Constructed Multiple Plasmonic Hotspots on an Individual Fractal to Amplify Broadband Hot Electron Generation. ACS Nano, 2021, 15, 10553-10564.	14.6	37
12	Achieving high strength and ductility in ODS-W alloy by employing oxide@W core-shell nanopowder as precursor. Nature Communications, 2021, 12, 5052.	12.8	87
13	Influence of minor Ti additive on the microstructure and mechanical properties of Mo based alloys. International Journal of Refractory Metals and Hard Materials, 2021, 99, 105599.	3.8	5
14	Accelerated sintering of high-performance oxide dispersion strengthened alloy at low temperature. Acta Materialia, 2021, 220, 117309.	7.9	30
15	Synthesis of W-Y2O3 alloys by freeze-drying and subsequent low temperature sintering: Microstructure refinement and second phase particles regulation. Journal of Materials Science and Technology, 2020, 36, 84-90.	10.7	85
16	Controlled synthesis of high-quality W-Y2O3 composite powder precursor by ascertaining the synthesis mechanism behind the wet chemical method. Journal of Materials Science and Technology, 2020, 36, 118-127.	10.7	58
17	W–Y2O3 composite nanopowders prepared by hydrothermal synthesis method: Co-deposition mechanism and low temperature sintering characteristics. Journal of Alloys and Compounds, 2020, 821, 153461.	5.5	30
18	Microstructure refinement in W–Y ₂ O ₃ alloys <i>via</i> an improved hydrothermal synthesis method and low temperature sintering. Inorganic Chemistry Frontiers, 2020, 7, 659-666.	6.0	19

#	Article	IF	CITATIONS
19	Influence of Yttrium Addition on the Reduction Property of Tungsten Oxide Prepared via Wet Chemical Method. Acta Metallurgica Sinica (English Letters), 2020, 33, 275-280.	2.9	12
20	The influence of phase formation routes on the microstructure and critical current density of Nb3Al superconductor prepared by mechanical alloying and subsequent sintering. Ceramics International, 2020, 46, 7977-7981.	4.8	1
21	Evaluation on elevated-temperature stability of modified 718-type alloys with varied phase configurations. International Journal of Minerals, Metallurgy and Materials, 2020, 27, 1123-1132.	4.9	18
22	Investigation on γ′ stability in CoNi-based superalloys during long-term aging at 900°C. Journal of Alloys and Compounds, 2020, 842, 155891.	5.5	11
23	Strain-modulated Ni3Al alloy promotes oxygen evolution reaction. Journal of Alloys and Compounds, 2020, 844, 156094.	5.5	21
24	Precipitation and coarsening behavior of γ′ phase in CoNi-base superalloy under different aging treatments. Vacuum, 2020, 175, 109247.	3.5	22
25	Enhanced critical current density in the low-temperature sintered Nb3Al superconductor with Sn doping. Intermetallics, 2020, 119, 106708.	3.9	6
26	Effect of Ti addition on high-temperature oxidation behavior of Co–Ni-based superalloy. Journal of Iron and Steel Research International, 2020, 27, 1179-1189.	2.8	21
27	The simultaneous improvements of strength and ductility in W–Y2O3 alloy obtained via an alkaline hydrothermal method and subsequent low temperature sintering. Materials Science & Engineering A: Structural Materials: Properties, Microstructure and Processing, 2020, 784, 139329.	5.6	36
28	Metal–organic framework derived copper catalysts for CO ₂ to ethylene conversion. Journal of Materials Chemistry A, 2020, 8, 11117-11123.	10.3	82
29	Influence of Al Addition Upon the Microstructure and Mechanical Property of Dual-Phase 9Cr-ODS Steels. Metals and Materials International, 2019, 25, 168-178.	3.4	7
30	The effect of Y2O3 on the grain growth and densification of W matrix during low temperature sintering: Experiments and modelling. Materials and Design, 2019, 181, 108080.	7.0	37
31	The synthesis of composite powder precursors <i>via</i> chemical processes for the sintering of oxide dispersion-strengthened alloys. Materials Chemistry Frontiers, 2019, 3, 1952-1972.	5.9	32
32	W-Y2O3 composite nanopowders prepared by freeze-drying method and its sintering characteristics. Journal of Alloys and Compounds, 2019, 806, 127-135.	5.5	40
33	Ultra-fine W–Y2O3 composite powders prepared by an improved chemical co-precipitation method and its interface structure after spark plasma sintering. Tungsten, 2019, 1, 220-228.	4.8	23
34	Microstructural evolution and constitutive models of 9CrMoCoB heat-resistant steel during high-temperature deformation. Journal of Iron and Steel Research International, 2019, 26, 1228-1239.	2.8	8
35	Hot deformation behaviors of a 9Cr oxide dispersion-strengthened steel and its microstructure characterization. International Journal of Minerals, Metallurgy and Materials, 2019, 26, 597-610.	4.9	10
36	Effect of deformation twinning on high-temperature performance of cold-rolled S31042 steel. Journal of Iron and Steel Research International, 2019, 26, 704-711.	2.8	2

#	Article	IF	CITATIONS
37	Effects of Isothermal Aging on Microstructure and Mechanical Property of Low-Carbon RAFM Steel. Acta Metallurgica Sinica (English Letters), 2019, 32, 1151-1160.	2.9	11
38	Formation mechanisms of Y–Al–O complex oxides in 9Cr-ODS steels with Al addition. Journal of Materials Science, 2019, 54, 7893-7907.	3.7	15
39	Coarsening behavior of γ′ precipitates in the γ'+γ area of a Ni3Al-based alloy. Journal of Alloys and Compounds, 2019, 771, 526-533.	5.5	86
40	The formation and evolution mechanism of amorphous layer surrounding Nb nano-grains in Nb-Al system during mechanical alloying process. Journal of Alloys and Compounds, 2019, 779, 175-182.	5.5	54
41	Helium bubble evolution and deformation of single crystal α-Fe. Journal of Materials Science, 2019, 54, 1785-1796.	3.7	8
42	Microstructural Feature and Evolution of Rapidly Solidified Ni3Al-Based Superalloys. Acta Metallurgica Sinica (English Letters), 2019, 32, 764-770.	2.9	9
43	Effect of annealing treatment on microstructure evolution and creep behavior of a multiphase Ni3Al-based superalloy. Materials Science & Engineering A: Structural Materials: Properties, Microstructure and Processing, 2019, 743, 623-635.	5.6	68
44	Eliminating bimodal structures of W-Y2O3 composite nanopowders synthesized by wet chemical method via controlling reaction conditions. Journal of Alloys and Compounds, 2019, 774, 122-128.	5.5	30
45	Evaluation of precipitation hardening in TiC-reinforced Ti2AlNb-based alloys. International Journal of Minerals, Metallurgy and Materials, 2018, 25, 453-458.	4.9	9
46	Precipitation and growth behavior of mushroom-like Ni3Al. Materials Letters, 2018, 211, 5-8.	2.6	18
47	Effects of aluminum and titanium on the microstructure of ODS steels fabricated by hot pressing. International Journal of Minerals, Metallurgy and Materials, 2018, 25, 1156-1165.	4.9	8
48	Morphology and quantitative analysis of O phase during heat treatment of hot-deformed Ti2AlNb-based alloy. International Journal of Minerals, Metallurgy and Materials, 2018, 25, 1191-1200.	4.9	11
49	Recent progress in friction stir welding tools used for steels. Journal of Iron and Steel Research International, 2018, 25, 477-486.	2.8	19
50	Preparation of ultra-fine grain W-Y2O3 alloy by an improved wet chemical method and two-step spark plasma sintering. Journal of Alloys and Compounds, 2017, 695, 2969-2973.	5.5	82
51	Evolution of Al-containing phases in ODS steel by hot pressing and annealing. Powder Technology, 2017, 311, 449-455.	4.2	19
52	Synthesis of nanosized composite powders via a wet chemical process for sintering high performance W-Y 2 O 3 alloy. International Journal of Refractory Metals and Hard Materials, 2017, 69, 266-272.	3.8	58
53	Effects of tantalum on austenitic transformation kinetics of RAFM steel. Journal of Iron and Steel Research International, 2017, 24, 705-710.	2.8	19
54	Microstructure Refinement in W-Y2O3 Alloy Fabricated by Wet Chemical Method with Surfactant Addition and Subsequent Spark Plasma Sintering. Scientific Reports, 2017, 7, 6051.	3.3	32

#	Article	IF	CITATIONS
55	Microstructural Characterization and Phase Separation Sequences During Solidification of Ni3Al-Based Superalloy. Acta Metallurgica Sinica (English Letters), 2017, 30, 949-956.	2.9	23
56	Microstructure characteristic and mechanical property of transformable 9Cr-ODS steel fabricated by spark plasma sintering. Materials and Design, 2017, 132, 158-169.	7.0	59
57	Damage micromechanics properties of bicrystalline α-Fe metals with two-voids. Physica B: Condensed Matter, 2017, 521, 275-280.	2.7	7
58	Effect of cold rolling and first precipitates on the coarsening behavior of γ″-phases in Inconel 718 alloy. International Journal of Minerals, Metallurgy and Materials, 2016, 23, 1087-1096.	4.9	22
59	Coarsening behavior of MX carbonitrides in type 347H heat-resistant austenitic steel during thermal aging. International Journal of Minerals, Metallurgy and Materials, 2016, 23, 283-293.	4.9	16
60	Phase Transformation Behavior and Microstructural Control of High-Cr Martensitic/Ferritic Heat-resistant Steels for Power and Nuclear Plants: A Review. Journal of Materials Science and Technology, 2015, 31, 235-242.	10.7	134
61	Effect of microstructure variation on the corrosion behavior of high-strength low-alloy steel in 3.5wt% NaCl solution. International Journal of Minerals, Metallurgy and Materials, 2015, 22, 604-612.	4.9	43
62	Morphology and structure evolution of Y2O3 nanoparticles in ODS steel powders during mechanical alloying and annealing. Advanced Powder Technology, 2015, 26, 1578-1582.	4.1	29
63	Effect of acicular ferrite on banded structures in low-carbon microalloyed steel. International Journal of Minerals, Metallurgy and Materials, 2014, 21, 1167-1174.	4.9	14
64	Structural refinement of 00Cr13Ni5Mo2 supermartensitic stainless steel during single-stage intercritical tempering. International Journal of Minerals, Metallurgy and Materials, 2014, 21, 279-288.	4.9	13
65	Precipitation behavior and martensite lath coarsening during tempering of T/P92 ferritic heat-resistant steel. International Journal of Minerals, Metallurgy and Materials, 2014, 21, 438-447.	4.9	23
66	Effect of indium addition on the microstructural formation and soldered interfaces of Sn-2.5Bi-1Zn-0.3Ag lead-free solder. International Journal of Minerals, Metallurgy and Materials, 2012, 19, 1029-1035.	4.9	12
67	In situ formation process and mechanism of bulk MgB ₂ before Mg melting. Journal of Materials Research, 2008, 23, 1840-1848.	2.6	7
68	Dynamic and quasi-static compressive performance of integral-forming aluminum foam sandwich. Journal of Iron and Steel Research International, 0, , .	2.8	2